Distinct Pathogenic Sequela in Rhesus Macaques Infected with CCR5 or CXCR4 Utilizing SHIVs

Janet M. Harouse,[1] Agegnehu Gettie,[1] Rei Chin How Tan,[1] James Blanchard,[2] Cecilia Cheng-Mayer[1]*

Infection of macaques with chimeric simian–human immunodeficiency virus (SHIV) provides an excellent in vivo model for examining the influence of envelope on HIV-1 pathogenesis. Infection with a pathogenic CCR5 (R5)–specific enveloped virus, $SHIV_{SF162P}$, was compared with infection with the CXCR4 (X4)–specific $SHIV_{SF33A.2}$. Despite comparable levels of viral replication, animals infected with the R5 and X4 SHIV had distinct pathogenic outcomes. $SHIV_{SF162P}$ caused a dramatic loss of $CD4^+$ intestinal T cells followed by a gradual depletion in peripheral $CD4^+$ T cells, whereas infection with $SHIV_{SF33A.2}$ caused a profound loss in peripheral T cells that was not paralleled in the intestine. These results suggest a critical role of co-receptor utilization in viral pathogenesis and provide a reliable in vivo model for preclinical examination of HIV-1 vaccines and therapeutic agents in the context of the HIV-1 envelope protein.

Despite recent advances in the treatment of AIDS, its severe global impact heightens the need for an efficacious vaccine against human immunodeficiency virus (HIV). Toward this end, significant efforts have been directed at developing animal models that faithfully mimic HIV-1 infection. Such systems provide a controlled setting not only for preclinical evaluation of antiviral compounds and vaccines but also for addressing issues related to viral pathogenesis. Several nonhuman primate models have been used to study HIV-1 infection. These include infection of macaques with simian immunodeficiency virus (SIV) (*1*); infection of chimpanzees and macaques with HIV-1 (*2*); infection of baboons and macaques with HIV-2 (*3*); and infection of macaques with chimeric envelope SHIV (simian–human immunodeficiency virus) constructed by substituting the *tat*, *rev*, and *env* coding regions of the pathogenic molecular clone SIV_{mac239} with corresponding regions from HIV-1 clones (*4*). Although each model provides insight about host and viral determinants of pathogenesis, the fidelity of these models has been limited by various parameters (*5*). For example, infection with pathogenic env SHIVs generally results in a profound state of immunodeficiency characterized by a precipitous loss in peripheral $CD4^+$ T cells (*6*). The kinetics of SHIV-induced lymphocyte loss differs significantly from that observed in either pathogenic SIV or HIV-1 infection (*7*), which raises doubts about the validity of this model system. The pathogenic SHIVs described thus far function with the CXCR4 (X4) co-receptor (*8*) or are dual-tropic, utilizing both CCR5 and CXCR4 (R5X4). The disease induced by these X4 and R5X4 SHIVs is more characteristic of late-stage HIV-1 infection or the rare infection of individuals who are homozygous for a 32–base pair (Δ32/Δ32) deletion in the gene encoding the CCR5 receptor (*9*). Development of a pathogenic CCR5 (R5)-specific SHIV might facilitate the preclinical analysis of candidate antiviral compounds and vaccines and reveal aspects of viral pathogenesis not observed in previously described animal model systems.

With the goal of developing an R5-specific pathogenic SHIV, we inoculated two rhesus macaques with a molecular clone $SHIV_{SF162}$ followed by three sequential blood–bone marrow transfusions into naïve macaques (*10*). This approach has been successfully used to generate X4 and dual-tropic pathogenic SHIVs (*11*). We collected longitudinal samples of peripheral blood and lymph node from each of the eight animals and analyzed the samples for plasma viremia and changes in T cell subsets (*12*). Significant amounts of viral replication were achieved during the acute phase of infection in passage 1 (P1) macaques with 10^6 viral RNA copies per milliliter of plasma. By 3 weeks postinfection (wpi), viremia began to decline and was not detected in either P1 animal after 6 weeks; nonetheless, proviral DNA and antiviral immune responses were still detected 11 months pi (*13*). Similar kinetics of viral replication were observed in passage 2 (P2) monkeys, albeit with slightly increased viral loads of 10^6 to 10^7 viral RNA copies per milliliter of plasma. Additional successive in vivo passage of $SHIV_{SF162}$, now designated $SHIV_{SF162P}$, significantly enhanced viral replication as demonstrated by viral peaks between 10^7 and 10^8 viral RNA copies per milliliter of plasma in both P3 (T353 and T833) and P4 (T378 and T642) macaques, and two animals sustained plasma viremia between 10^4 and 10^5 viral RNA copies per milliliter of plasma for over 11 months (Fig. 1A). Concomitant with peak viral load (2 wpi) was a moderate drop in the absolute number of $CD4^+$ peripheral blood mononuclear cells (PBMCs). However, this cell population rebounded to near baseline values at 4 to 6 wpi (Fig. 1B).

To determine whether $SHIV_{SF162P}$ maintained CCR5 specificity, we used PBMCs purified from a homozygous Δ32/Δ32 seronegative donor for in vitro studies. Results showed that, similar to the parental $SHIV_{SF162}$, viruses isolated from P4 animals [T378, lymph node mononuclear cell (LNMC) isolate; T642, PBMC isolate] 2 weeks after infection did not infect human PBMCs lacking CCR5 surface expression, whereas the X4-specific $SHIV_{SF33A.2}$ clone readily infected both wild-type and Δ32/Δ32 PBMCs (Fig. 2). Additionally, using HOS cells engineered to express the CD4 protein along with specific co-receptors, we found that P4 viruses were able to infect GHOST cells expressing the CCR5 protein but not those expressing CXCR4, BOB/GPR15, or Bonzo/STRL33

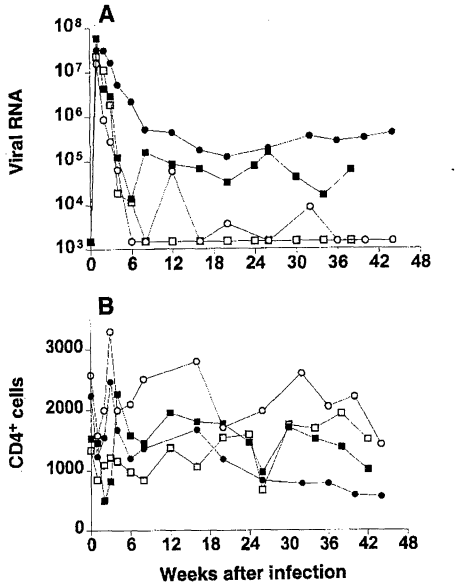

Fig. 1. Peripheral blood was collected in EDTA at weekly intervals and separated into plasma and cellular compartments. (**A**) Copies of viral RNA in plasma per milliliter of plasma determined by bDNA analysis (Chiron). P3 macaques, T353 (solid circles) and T833 (open circles); P4 macaques, T378 (solid squares) and T642 (open squares). (**B**) Absolute number of $CD3^+$ $CD4^+$ cells per microliter of blood as determined by TruCount FACS analysis.

[1]Aaron Diamond AIDS Research Center, The Rockefeller University, 455 First Avenue, 7th Floor, New York, NY 10016, USA. [2]Tulane Regional Primate Research Center, Tulane University Medical Center, 18073 Three Rivers Road, Covington, LA 70433, USA.

*To whom correspondence should be addressed. E-mail: cmayer@Adarc.org

(*13, 14*). Collectively, these data strongly suggest that, despite vigorous in vivo replication of $SHIV_{SF162P}$, viruses isolated from infected animals maintain CCR5 specificity with no evidence of expanded co-receptor utilization.

The transient loss in peripheral $CD4^+$ T cells in P3 and P4 animals early after infection (Fig. 1B) is in sharp contrast to the profound and sustained depletion that occurs during primary infection with previously described X4- and dual-tropic SHIVs (*6*). A comparison of the viral load and peripheral T cell ratios between a representative macaque infected with $SHIV_{SF33A}$ (*15*) and the P3 $SHIV_{SF162P}$-infected animal T353 illustrates a striking difference in $CD4^+$ cell loss in these macaques despite comparable levels of viral replication (Fig. 3). In light of recent reports that indicate the gastrointestinal tract, and not peripheral lymphoid tissue, is the major site for replication of SIV during primary infection, we analyzed T cell populations within the gut-associated lymphoid tissue (GALT) in the P4 macaques (*16*). Jejunal biopsies and mesenteric nodes were obtained from P4 macaques by surgical resectioning of the intestinal tract 2 weeks after viral infection (*17*). Intestinal epithelia and lamina propria lymphocytes (LPLs) were isolated from fresh jejunal tissue (*18*) and LNMCs were isolated from both colonic and inguinal lymph nodes followed by three-color flow cytometry analysis for expression of CD3, CD4, and CD8. During acute infection, both P4 animals suffered depletion in the $CD4^+$ LPL subset (T378, 8%; T642, 7%; Fig. 4A). This severe diminution in $CD4^+$ T cells is unique to the GALT as lymphocytes isolated concurrently from blood or lymph nodes showed moderate changes in the percentage of $CD4^+$ cells. To determine whether the $CD4^+$ T cell subset was restored in jejunal tissue, we performed a follow-up analysis on the same P4 animals during chronic infection (26 wpi). After nearly 6 months of infection, the percentage of $CD4^+$ T cells detected in the jejunum (T378, 24% $CD4^+$; T642, 14% $CD4^+$) had regenerated slightly compared with amounts during acute infection (Fig. 4, B and C); however, the percentage of $CD4^+$ cells within LPLs was diminished compared with published uninfected control values (*18*). To further examine the pathogenicity of $SHIV_{SF162P}$, we inoculated four naïve animals intravenously with cell-free virus recovered from PBMCs of macaque T378 (P4) and then analyzed the tissue. These animals also had high levels of plasma viremia accompanied by depletion of $CD4^+$ jejunal LPLs (9.7% ± 5.5%) with minimal changes in circulating $CD4^+$ T cells at 2 wpi (*13*). Thus, similar to animals infected with CCR5 utilizing SIV, animals infected with $SHIV_{SF162P}$ had a profound loss of $CD4^+$ T cells within the gastrointestinal tract while maintaining a

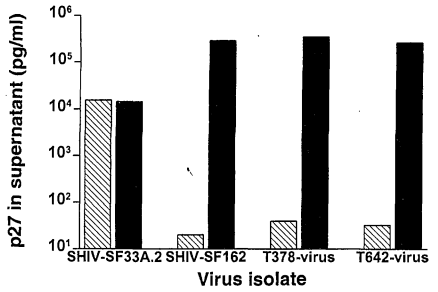

Fig. 2. Virus recovered from P4 animals 2 weeks after infection was examined for replication in PBMCs isolated from a CCR5 wild-type donor (CCR5 +/+; solid squares) and a donor homozygous for Δ32 (CCR5 −/−; hatched squares). Culture supernatants were collected 10 days after infection and analyzed for $p27^{gag}$ content by antigen ELISA (Cellular Products, Buffalo, New York).

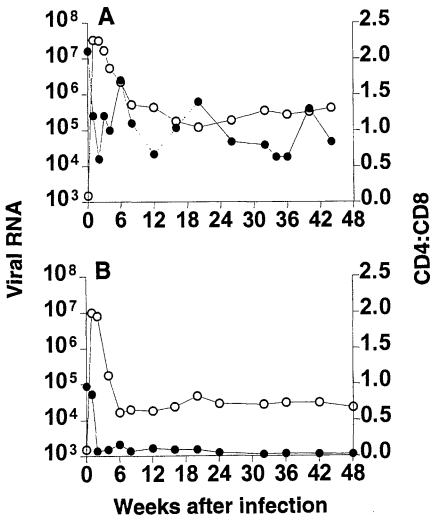

Fig. 3. Comparison of plasma viremia (viral RNA per milliliter of plasma) (open circles) and CD4-CD8 T cell ratios (solid circles) during primary infection with $SHIV_{SF162P}$ (**A**) and $SHIV_{SF33A}$ (**B**).

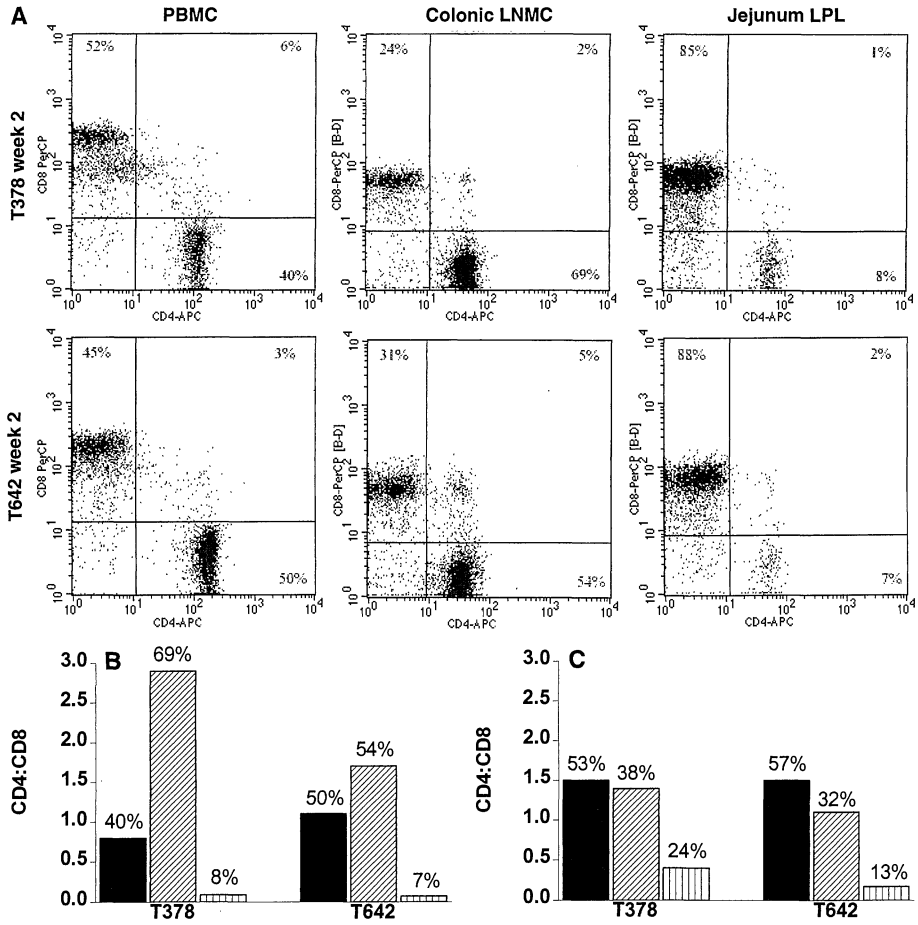

Fig. 4. (**A**) Three-color flow cytometry dot plots comparing lymphocytes isolated from the peripheral blood (PBMCs), colonic lymph node (LNMCs), and intestinal lamina propria (LPLs) 2 weeks after infection with $SHIV_{SF162P}$. (**Top**) Cells obtained from P4 animal T378; (**bottom**) cells from P4 animal T642. Dot plots were generated by first selecting lymphocyte population and then selecting $CD3^+$ T cells. Analysis of CD4-CD8 T cell ratios in lymphoid tissue at 2 weeks in peripheral blood (PBMCs; solid squares), colonic lymph node (LNMCs; hatched squares), and intestinal lamina propria (LPLs; striped squares) (**B**), and at 26 weeks in $SHIV_{SF162P}$-infected macaques (**C**). The actual percentage of $CD4^+$ T lymphocytes in each compartment is given in (B) and (C).

relatively high number of peripheral $CD4^+$ T cells. Similarly, analysis of asymptomatic HIV-1 patients suggests that $CD4^+$ T cell depletion within the intestinal mucosa precedes the depletion in peripheral blood (*19*).

To further explore differential pathogenesis associated with X4 and R5 viruses, we determined T cell loss in GALT of X4-infected animals by means of a recently developed and characterized infectious molecular clone of $SHIV_{SF33A}$ designated $SHIV_{SF33A.2}$ (*13*). We inoculated two macaques intravenously with $SHIV_{SF33A.2}$ and subjected them to the same blood, lymph node, and jejunal sampling procedures as described for the P4 $SHIV_{SF162}$ animals. As observed with the parental isolate $SHIV_{SF33A}$ and other pathogenic X4 or R5X4 SHIVs (*6*), animals infected with the X4-specific $SHIV_{SF33A.2}$ had a profound loss of circulating $CD4^+$ T cells within 2 weeks of infection. Moreover, in marked contrast to $SHIV_{SF162P}$ is the absence of severe $CD4^+$ T cell depletion in the GALT of $SHIV_{SF33A.2}$-infected macaques (E239, 32%; G901, 49%) (Fig. 5). Although we did not determine the amount of viral infection in mucosal tissues, $SHIV_{162P}$- and $SHIV_{SF33A.2}$-infected animals had comparable levels of plasma viremia.

Despite viral loads comparable to that of the pathogenic X4-utilizing $SHIV_{SF33A}$ and significant steady-state level of viral replication, the characteristic rapid and sustained inversion of the peripheral CD4-CD8 T cell ratio did not occur in late passaged $SHIV_{SF162P}$-infected animals (Fig. 3). Rather, these animals had a gradual loss in the absolute number of peripheral $CD4^+$ T cells reminiscent of most HIV-1 and SIV infections. However, analysis of LPLs purified from jejunal tissue revealed a severe depletion of mucosal $CD4^+$ T cells within 2 weeks of inoculation, demonstrating that $SHIV_{SF162P}$ is intrinsically pathogenic. Thus, productive infection with $SHIV_{SF162P}$ results in a pathogenic sequela similar to SIV infection in macaques rather than previously described pathogenic SHIV infections. This is further illustrated by our finding that, although macaques infected with the X4-specific molecular clone $SHIV_{SF33A.2}$ suffer a profound loss of circulating $CD4^+$ T cells, they do not undergo severe depletion in jejunal LPLs immediately after infection. These marked differences in viral pathogenesis occur despite similar levels of sustained plasma viremia. The most obvious difference between $SHIV_{SF162P}$ and $SHIV_{SF33A.2}$ is co-receptor utilization that dictates the target cell of infection of each virus. It is known that CCR5 and CXCR4 expression varies in different cell types and at different stages of human T cell development (*20*). The depletion of $CD4^+$ lymphocytes within the GALT during SIV infection may be due to the high percentage of activated memory $CD4^+$ T cells within the gut (*16*) that preferentially express CCR5 co-receptor (*20*). The absence of $CD4^+$ T cell loss in jejunal LPLs of X4-infected animals therefore may reflect the lack of susceptible host target cells within the intestinal mucosa. In this regard, preliminary analysis of CXCR4 expression in various lymphoid compartments of $SHIV_{SF33A.2}$-infected macaques indicates that, although comparable percentages of $CD3^+$ $CD4^+$ $CXCR4^+$ cells are present in these anatomically distinct compartments, the level of CXCR4 expression is significantly lower in the $CD3^+$ LPLs than in LNMCs and PBMCs (*13*). Similar analysis with antibodies that recognize macaque CCR5 and markers of T cell development and differentiation will likely shed light on the mechanisms that underlie the preferential loss of $CD4^+$ T cells from distinct compartments of $SHIV_{SF162P}$-infected macaques. Thus, our findings suggest that target cell and tissue tropism, as influenced by differential co-receptor expression, may have profound implications on viral pathogenesis and subsequent host disease course.

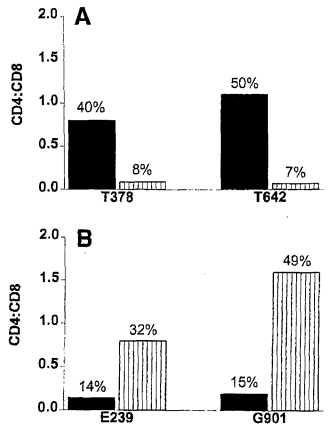

Fig. 5. Comparison of T cell ratios in PBMC (solid squares) and jejunal LPL (striped squares) subsets 2 weeks after infection with $SHIV_{SF162P}$ (**A**) and $SHIV_{SF33A.2}$ (**B**). The actual percentage of $CD4^+$ T lymphocytes in each compartment is given.

The availability of pathogenic R5- and X4-specific envelope SHIVs that replicate with similar kinetics and to comparable levels provides the tools that are necessary to answer important questions related to viral pathogenesis, transmission, adaptation, and evolution. Although our data suggest that differential co-receptor utilization of $SHIV_{SF162P}$ and $SHIV_{SF33A.2}$ significantly alters viral pathogenesis, it does not a priori indicate that co-receptor utilization is the sole determinant of viral pathogenesis. Co-receptors mediate viral entry into target cells, but productive HIV infection requires cellular activation (*21*). Thus, further phenotypic analysis of the host cells that are susceptible to productive infection with $SHIV_{SF162P}$ and $SHIV_{SF33A.2}$ may provide insight into these important issues of pathogenesis. Additionally, the $SHIV_{SF162P}$ and $SHIV_{SF33A}$ animal model system described will be instrumental in addressing the long debated issues of preferential R5 transmission and phenotypic switch. Whether R5 viruses are exclusively selected or amplified during viral transmission and subsequently evolve into X4 viruses, perhaps to evade host immune responses or, alternatively, whether both R5 and X4 viruses are transmitted but X4 virus is sequestered early after transmission and eventually outgrows R5 virus can now be examined (*22*). An understanding of these and other interactions between HIV-1 proteins and host target cells should lead to improved understanding of viral pathogenesis and should help in development of effective vaccine and therapeutic candidates.

References and Notes

1. R. C. Desrosiers, *Annu. Rev. Microbiol.* **42**, 607 (1988); J. Overbaugh, P. A. Luciw, E. A. Hoover *AIDS* **11** (suppl. A), S47 (1997).
2. H. J. Alter *et al.*, *Science* **226**, 549 (1984); P. Fultz *et al.*, *J. Virol.* **58**, 116 (1986); M. B. Agy *et al.*, *ibid.* **257**, 103 (1992)
3. P. Putkonen *et al.*, *J. AIDS* **2**, 366 (1989); S. W. Barnett, K. K. Murthy, B. G. Herndier, J. A. Levy, *Science* **266**, 642 (1994).
4. J. Li, C. I. Lord, W. Haseltine, N. L. Letvin, J. Sodroski, *J. AIDS* **5**, 639 (1992); S. Sakuragi *et al.*, *J. Gen. Virol.* **73**, 2983 (1992); P. A. Luciw, E. Pratt-Lowe, K. E. S. Shaw, J. A. Levy, C. Cheng-Mayer, *Proc. Natl. Acad. Sci. U.S.A.* **92**, 7490 (1995); K. A. Reimann *et al.*, *J. Virol.* **70**, 3198 (1996).
5. N. L. Letvin, *Science* **280**, 1875 (1998).
6. R. Shibata *et al.*, *J. Infect. Dis.* **176**, 362 (1997); K. A. Reimann *et al.*, *J. Virol.* **70**, 6922 (1996); S, V. Joag *et al.*, *ibid.*, p. 3189; J. M. Harouse *et al.*, *Virology* **248**, 95 (1998).
7. M. T. Niu, D. S. Stein, S. M. Schnittman, *J. Infect. Dis.* **168**, 1490 (1993); M. A. Nowak *et al.*, *J. Virol.* **71**, 7518 (1997); T. Schneider *et al.*, *Gut* **37**, 524 (1995).
8. Y. Feng, C. C. Broder, P. E. Kennedy, E. A. Berger, *Science* **272**, 872 (1996).
9. N. L. Michael *et al.*, *J. Virol.* **72**, 6040 (1998); I. Theodoru, L. Meyer, M. Magierowska, C. Katlama, C. Rouzioux, *Lancet* **349**, 1219 (1997); R. Biti *et al.*, *Nature Med.* **3**, 252 (1997); R. Liu *et al.*, *Cell* **86**, 367 (1996).
10. Serial passage of the molecular clone $SHIV_{SF162}$ was performed as follows: we inoculated two juvenile *Macaca mulatta* (P1) intravenously with 10^4 median tissue culture infectious dose of cell-free $SHIV_{SF162}$ propagated in human PBMCs [A. Luciw *et al.*, *Proc. Natl. Acad. Sci. U.S.A.* **92**, 7490 (1995)]. Two weeks after inoculation 10 ml of peripheral blood and 5 ml of bone marrow aspirate were collected from each animal, combined, and used to transfuse two naïve recipients (P2). This inoculation schedule was performed two more times in naïve recipients group P3 and P4. All clinical procedures were performed in accordance with Institutional Animal Care and Use Committee (IACUC) guidelines at the Tulane Regional Primate Research Center.
11. S. V. Joag *et al.*, *J. Virol.* **70**, 3189 (1996); K. A. Reimann *et al.*, *ibid.*, p. 6922.
12. Plasma was clarified from EDTA-treated whole blood by centrifugation. We then subjected clarified samples to p27 antigen enzyme-linked immunosorbent assay (ELISA) (Retro-TEK SIV p27 antigen ELISA; Cellular Products, Buffalo, NY), branched DNA (bDNA) analysis (Chiron, Emeryville, CA), and strip immunoblot assay to detect humoral immune responses (Chiron RIBA HIV-1/HIV-2 SIA, Chiron). To analyze T cell subsets we used the following human monoclonal antibodies (mAb): Leu-5b-FITC (fluorescein isothio-

cyanate), Leu-3a-PE (phycoerythrin), and Leu-2a-PerCP (peridinin chlorophyll protein), which recognize the CD2, CD4, and CD8 molecules, respectively (Becton Dickinson, San Jose, CA); 7E14-APC (allophycocyanin), which recognizes the CD4 protein (Exalpha, Boston, MA); and 12G5-PE, which recognizes the CXCR4 protein (Pharmingen, San Diego, CA). The mAb FN-18-FITC, which recognizes the monkey CD3 molecule, was also used (Biosource International, Camarillo, CA). Absolute CD4 and CD8 cell counts were measured with TruCount absolute count tubes (Becton Dickinson, Mountainview, CA) according to the manufacturer's instructions. Flow cytometry analysis was performed with the FACS Calibur.

13. J. M. Harouse and C. Cheng-Mayer, unpublished data.
14. H. Deng, D. Unutmaz, V. N. Kewal-Ramani, D. R. Littman, *Nature* **388**, 296 (1997); M. Farzan *et al.*, *J. Exp. Med.* **186**, 405 (1997); G. Alkhatib *et al.*, *Nature* **388**, 238 (1997).
15. J. M. Harouse *et al.*, *Virology* **248**, 95 (1998).
16. R. S. Veazey *et al.*, *Science* **280**, 427 (1998); J. J. Mattapallil *et al.*, *J. Virol.* **72**, 6421 (1998); Z. Smit-McBride *et al.*, *J. Virol.* **72**, 6646 (1998).
17. Jejunal resectioning and anastomosis were performed by excising about 20 cm of intestinal tissue [D. Slatter, *Textbook of Small Animal Surgery* (Saunders, Philadelphia, ed. 2, 1993), vol. 1]. We dissected Colonic nodes from colonic mesentery and took ileal wedge biopsies from the antimesenteric side of the intestine followed by closure with a nylon suture. Surgical samples were processed within 30 min of the procedure. All surgical procedures were performed on anesthetized animals and were approved by IACUC.
18. R. S. Veazey *et al.*, *Clin. Immunol. Immunopathol.* **82**, 230 (1997). In this study, the range of $CD4^+$ jejunal LPLs in normal adult rhesus macaques was 34.3% to 56.9%, with a corresponding CD4-CD8 ratio of 0.88 ± 0.22 ($n = 4$).
19. T. Schneider *et al.*, *Gut* **37**, 524 (1995).
20. C. Bleul, L. Wu, J. A. Hoxie, T. A. Springer, C. R. Mackay, *Proc. Natl. Acad. Sci. U.S.A* **94**, 1925 (1997); R. D. Berkowitz, K. P. Beckerman, T. J. Schall, J. M. McCune, *J. Immunol.* **161**, 3702 (1998).
21. J. A. Zack *et al.*, *Cell* **61**, 213 (1990).
22. P. Trivedi *et al.*, *J. Virol.* **70**, 6876 (1996); T. Zhu *et al.*, *ibid.*, p. 3098.
23. Supported in part by National Institutes of Health grants AI41945 and CA72822. We thank D. D. Ho, R. Connor, R. Liu, S. Monard, and J. Segal (Aaron Diamond AIDS Research Center); R. Bohm, L. Martin, M. Ratterree, and the animal care staff at Tulane Regional Primate Research Center; R. Koup (University of Texas, Southwestern); P. J. Dailey, L. Sawyer, and J. Booth (Chiron Diagnostics); and R. Veazey (New England Regional Primate Research Center).

12 February 1999; accepted 26 March 1999

Chemokine Up-Regulation and Activated T Cell Attraction by Maturing Dendritic Cells

H. Lucy Tang and Jason G. Cyster*

Langerhans' cells migrating from contact-sensitized skin were found to up-regulate expression of macrophage-derived chemokine (MDC) during maturation into lymph node dendritic cells (DCs). Naïve T cells did not migrate toward MDC, but antigen-specific T cells rapidly acquired MDC responsiveness in vivo after a subcutaneous injection of antigen. In chemotaxis assays, maturing DCs attracted activated T cells more strongly than naïve T cells. These studies identified chemokine up-regulation as part of the Langerhans' cell maturation program to immunogenic T cell–zone DC. Preferential recruitment of activated T cells may be a mechanism used by maturing DCs to promote encounters with antigen-specific T cells.

Skin DCs, or Langerhans' cells (LCs), form an extensive network in the epidermis, and upon exposure to noxious stimuli such as lipopolysaccharide (LPS) or to contact sensitizers such as fluorescein isothiocyanate (FITC), they enter lymphatics and migrate into T cell zones of lymph nodes to become interdigitating DCs (*1*). For mature DCs to function in an immunogenic manner, it is important that they rapidly interact with antigen-specific T cells. One mechanism that may enhance encounters between DCs and T cells is for DCs to produce T cell–attracting chemokines. Although DCs express several chemokines (*2–5*), it has not been established whether immature DCs such as LCs up-regulate chemokine expression during in vivo maturation to immunogenic DCs.

Macrophage-derived chemokine (MDC) is highly expressed in lymphoid tissues (*5–8*). To characterize its expression in more detail, we isolated the mouse MDC homolog and used it to probe lymphoid tissues by in situ hybridization (*9*). Multiple strongly hybridizing cells were identified in T cell zones of lymph nodes (Fig. 1B), whereas only occasional cells hybridized in the spleen (Fig. 1A). Frequently, the MDC-expressing cells were concentrated in regions of the T cell zone proximal to follicles (Fig. 1B), which are areas rich in DCs (*1*), and under higher magnification, they demonstrated a dendritic morphology (Fig. 1C). Consistent with the in situ data and with findings by others (*5–8*), Northern (RNA) blot analysis showed that MDC was highly expressed in lymph node DCs (Fig. 1D) and was undetectable in DC-depleted lymph nodes or in peritoneal macrophages (Fig. 1D). To test for the production of MDC protein, we incubated purified lymph node DCs in vitro to allow chemokine secretion, and we tested the culture supernatant for the attraction of mouse CC-chemokine receptor 4 (CCR4)–transfected cells (*10–13*). A chemotactic response was observed with transfected but not with control cells (Fig. 1E). In addition to making MDC, we found, in preliminary studies (*14*), that lymph node DCs express thymus- and activation-regulated chemokine (TARC), which is a second CCR4 ligand (*15*), and it is possible that TARC contributes to the CCR4 cell attractant activity made by DCs.

After the exposure of skin to contact sensitizers, LCs migrate to lymph nodes but do not enter circulation or migrate to the spleen (*1, 16, 17*), raising the possibility that the MDC-expressing DCs in lymph nodes might be LC derived. We therefore tested whether exposure to the contact sensitizer FITC resulted in changes in lymph node MDC expression. One day after skin was painted with FITC (*18*), MDC expression in draining lymph nodes was increased threefold (Fig. 2A), and it remained elevated over the next 2 days (Fig. 2A). In contrast, no increase in MDC occurred in the spleen after an intravenous injection of LPS (Fig. 2A), a treatment that promotes the migration of DCs from the splenic marginal zone to the T cell zone (*19*). In agreement with previous studies (*20*), $FITC^+$ major histocompatability complex (MHC) class II^+ DCs could be detected among cells from lymph nodes draining a site of skin painted with FITC, and these DCs were absent from nondraining nodes (Fig. 2B). A microscopic analysis of isolated DCs showed that the FITC was concentrated within intracellular compartments (Fig. 2C). When day one draining lymph nodes were sectioned and stained to identify B and T cell zones, small numbers of brightly fluorescent $FITC^+$ cells could be identified within the T cell zone but not in follicles (Fig. 2D). Combining this technique of tracking migrating DCs with in situ hybridization for MDC (*9*), we found that it was possible to establish that many of the FITC-bearing cells in the T cell zone were strongly positive for MDC expression (Fig. 2E). Reverse transcriptase–polymerase chain reaction (RT-PCR) analysis of sorted $FITC^+$ lymph node DCs (*21*) confirmed that MDC was expressed in these cells (Fig. 3A). In contrast, EBI-1 ligand chemokine (ELC), a chemokine expressed constitutively by a subset of T cell zone DCs (*4*), was not detectable among $FITC^+$ DCs (Fig. 3A).

Department of Microbiology and Immunology, University of California at San Francisco, San Francisco, CA 94143, USA.

*To whom correspondence should be addressed. E-mail: cyster@itsa.ucsf.edu